Nano-granular Co-Fe-Al-O Soft Ferromagnetic Thin Films for RF Electromagnetic-noise Filters

Jae Cheon Sohn[a]
Nano Device Research Center, Korea Institute of Science and Technology, Hawolgok 2-dong, Seongbuk-gu, Seoul 136-791, Korea

Dong Jin Byun
Department of Materials Science and Engineering, Korea University, Anam-dong 5-ga, Seongbuk-gu, Seoul 136-701, Korea

[a]E-mail : jcsohn@kist.re.kr

(Received November 15 2005, Accepted January 11 2006)

Co-Fe-Al-O nano-granular thin films with high electrical resistivity, fabricated by radio frequency magnetron sputtering under an Ar+O_2 atmosphere, are found to show good soft magnetic properties in the GHz frequency range. The real part value of the relative permeability is 260 at low frequencies and this value is maintained up to the GHz frequency range. A non-integrated type noise filter on a coplanar waveguide transmission line is demonstrated by using the Co-Fe-Al-O nano-granular thin film with the dimensions of 4 mm (l) × 4 mm (w) × 0.1 μm (t). The insertion loss is very low being less than 0.3 dB and this low value is maintained up to 2 GHz. At a ferromagnetic resonance frequency of 3.3 GHz, the degree of noise suppression is measured to be 3 dB. This level of noise attenuation is small for real applications, but there is much room for further improvement by increasing the magnetic volume and integrating the magnetic thin film into the CPW transmission line.

Keywords : Nano-granular thin film, Co-Fe-Al-O, Electromagnetic-noise filter, Coplanar transmission line, Radio frequency

1. ITRODUCTION

With a large volume of information and a variety of communication media such as mobile telephones and satellite broadcasting devices, the development of high-frequency devices is of significant practical importance. The goal of mobile/wireless communications in the coming years will be to allow users to access the global network at any time, without regard to mobility or location. Continued developments in satellite communications, fiber-optic and digital microwave radio communications are aimed at this goal. Many component devices such as band-pass filters, duplexers and resonators must also conform to high-frequency bands. Although the high operational frequency in electronic devices can improve their performance, it can be a source of electromagnetic noise. Developing countermeasures for suppressing electromagnetic noise in the frequency range of several hundreds MHz to several GHz have therefore become important technical issues. In the past, various types of suppression devices were considered to tackle the electromagnetic noise problem. In recent years, noise filters using magnetic materials were developed and the results were reported to be satisfactory[1,2]. In these devices, magnetic materials play important roles in suppressing electromagnetic noise through the loss generation of ferromagnetic resonance (FMR).

Since the frequency of the noise generated from current radio frequency (RF) wireless communication devices is usually very high being in the GHz range, the magnetic materials should exhibit a high FMR frequency (f_R). A high f_R can be obtained at a large saturation magnetization ($4\ \pi M_s$) and anisotropy field (H_K), according to the equation $f_R = (\gamma/2\ \pi)(4\ \pi M_S H_K)^{1/2}$ obtained for a single domain magnetic thin film. Here γ is the gyromagnetic ratio. Another important requirement is a high electrical resistivity (ρ); otherwise, the eddy current losses are extremely large in the GHz frequency range. Of course, a high relative permeability (μ_r) is desirable, since μ_r is directly related with the level of noise suppression. In the case of bulk ferrites with a

small $4\pi M_s$, μ_r is low and also f_R is relatively low. This is the reason why bulk ferrites are not widely used in high-frequency applications, although they are mostly insulators. On the other hand, ferromagnetic metals generally have a large μ_r due to their large $4\pi M_s$ and relatively small H_K. However, the main limiting factor is a small ρ value, causing large eddy current losses. So, ferromagnetic metals are not suitable for practical use in the high-frequency region. Consequently, magnetic materials suitable for high-frequency RF applications should have a large $4\pi M_s$ and a high H_K, thereby increasing f_R, as well as a large ρ, thereby reducing eddy current losses[3-5].

Recently developed nano-granular magnetic thin films were known to meet these requirements. The nano-granular thin films consist of nano-meter scale ferromagnetic grains and these grains are usually completely separated by an insulating phase. This micro-structural feature is important to achieve a high ρ. Exchange coupling between nano-granules still exists across the insulating boundary. This is a necessary condition for the random anisotropy model by which the effective magneto-crystalline anisotropy is greatly reduced, resulting in excellent magnetic softness[6]. Thus, it is expected that the nano-granular magnetic thin films have a high μ_r and low eddy current losses even in the high frequency region.

Previous work on Fe-based nano-granular magnetic thin films has shown a relatively high $4\pi M_s$, but small H_K. This is insufficient for high frequency operation, because the resulting f_R is not high enough for GHz-level frequency applications[7-9]. On the other hand, Co-based magnetic thin films show a small μ_r due to a relatively small $4\pi M_s$ and large H_K when compared with Fe-based magnetic thin films[10,11]. Co-Fe-based nano-granular alloys have combined merits of respective Fe- and Co-based alloys. The micro-structural feature that Co-Fe grains are completely surrounded with an insulating phase is essential to the realization of a high ρ. Co-Fe-Al-O thin films with (Co,Fe) nano-grains in an amorphous Al-O matrix were reported to show very good soft magnetic properties even in the GHz range[12]. The thin films also exhibit a small coercivity, mainly due to a very small (nano-crystalline) (Co,Fe) grain size. From these excellent high-frequency soft magnetic properties of nano-granular Co-Fe-Al-O thin films, large electromagnetic noise attenuation is expected to occur on a coplanar waveguide (CPW) transmission line device.

In this study, nano-granular Co-Fe-Al-O thin films are tested as a non-integrated noise filter on a CPW transmission line. The non-integrated noise filter is constructed by simply placing a Co-Fe-Al-O thin film on a CPW transmission line. Usually, an insulating layer is disposed between a CPW line and a magnetic thin film in order to prevent electrical short. But, no insulator is placed in this study, because the value of ρ of the present Co-Fe-Al-O thin films is considered to be high enough to avoid electrical short, at least in a non-integrated type device. Here, the noise suppression characteristics are evaluated over a wide-frequency range and then the possibility as a high-frequency noise filter is discussed.

2. EXPERIMENTAL

Co-Fe-Al-O nano-granular thin films with a thickness of approximately 0.1 μm were fabricated by RF magnetron sputtering in an O_2+Ar atmosphere. The background pressure was better than 7×10^{-7} Torr. The O_2 flow ratio was varied mainly to change the oxygen content in the thin films. Co-Fe-Al composite targets composed of a Co-Fe alloy target and Al chips were used The films were grown on Si substrates in a static field of 1 kOe to induce uniaxial magnetic anisotropy. The microstructure was examined by x-ray diffraction (XRD) using Cu$K\alpha$ radiation and by high-resolution transmission electron microscopy (HRTEM) combined with nano-beam electron diffraction. The overall composition of the films was determined by electron probe microanalysis (EPMA) and Auger electron spectroscopy (AES). The composition of nano-grains was mainly measured by energy dispersive x-ray spectroscopy (EDX) combined with HRTEM with a beam diameter of 2 nm. Magnetic properties were evaluated with a vibrating sample magnetometer (VSM). The magnitude of f_R was obtained from the frequency profile of complex permeability, $\mu_r = \mu_r' + j\mu_r''$, measured up to 9 GHz with a pick-up coil type permeameter. The value of ρ was obtained by using the conventional four-probe method.

A Co-Fe-Al-O thin film deposited on a silicon substrate was mounted on top of a CPW transmission line. It is noted that the film surface, not the Si substrate, is in contact with a CPW line. The proximity between a magnetic thin film and a CPW line can be varied with an applied pressure, but, in the present study, no intentional pressure was applied. The dimensions of the film are 4 mm (l) × 4 mm (w) × 0.1 μm (t). Following the Muller and Hillberg equations[13], the CPW transmission line with a characteristic impedance of 50 Ω is designed for a signal line width of 50 μm and a thickness of 3 μm on a 7059 corning glass substrate. The detailed structure of the CPW transmission line is shown in Fig. 1. The S-parameters (S_{11} and S_{21}) were measured with a HP 8720D network analyzer in the frequency range of 0.1 to 20 GHz. Two ground-signal-ground (GSG) pin type wafer probes were in mechanical contact with both ends of the CPW transmission line. A brief explanation of the

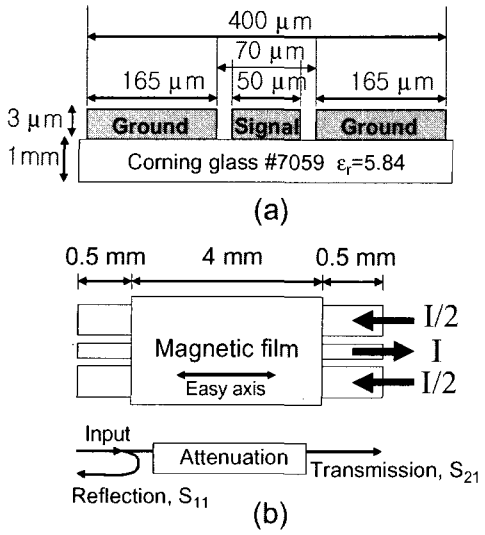

Fig. 1. (a) The cross-sectional view of the CPW transmission line (with detailed dimensions) used in this work. (b) A top view of a noise suppressor showing a magnetic film on top of the CPW transmission line. Note that the dimensions are not in a proper scale.

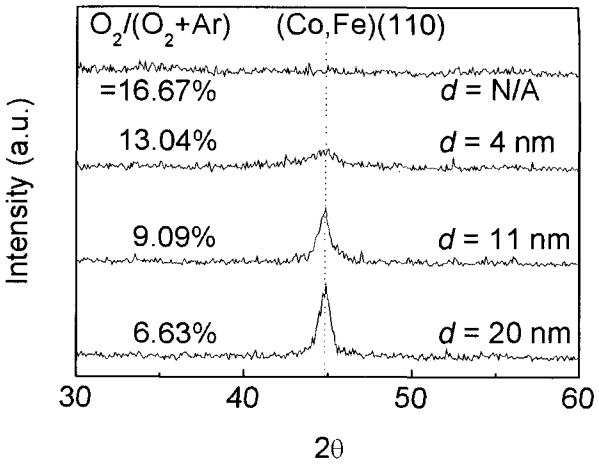

Fig. 2. XRD patterns of as-deposited Co-Fe-Al-O films.

S-parameters is given as follows (see Fig. 1(b)). An input signal and/or noise is introduced from the left-hand side and is partly reflected at the left-hand end of the magnetic film. This reflected signal is called S_{11}, the reflection scattering parameter. The counterpart goes into the magnetic film portion where a certain degree of attenuation occurs due to FMR losses. Then the transmission signal or noise, called the transmission scattering parameter (S_{21}), reaches the right-hand end of the CPW line.

3. RESULTS AND DISCUSSION

3.1 Microstructure

XRD patterns of as-deposited Co-Fe-Al-O films at various O_2 flow ratios are shown in Fig. 2. The input power (200 W) and the sputtering pressure (5 mTorr) are fixed, but the O_2 flow ratio is varied from 6.63 to 16.67 % and indicated in the figure. Also indicated is the grain diameter (*d*), which was determined by using the Scherrer formula. The (110) diffraction peak corresponding to the bcc (Co,Fe) phase is observed at low O_2 flow ratios of 6.63, 9.09 and 13.04 %, but it is absent at the highest O_2 flow ratio of 16.67 %. No peaks related with oxides are observed, indicating that Al-O is present as an amorphous phase and (Co,Fe) grains are not oxidized, at least at an substantial amount to be detected by XRD. The absence of the bcc (Co,Fe) phase at the highest O_2 flow ratio may indicate that the amount of the bcc (Co,Fe) phase is significantly reduced at this high O_2 flow ratio. The width of the (110) peak increases and the height decreases with increasing O_2 flow ratio, indicating a smaller grain size at a higher O_2 flow ratio. The reduction of the grain size with the increase of the O_2 flow ratio is in agreement with the previous observation [14] and this is because the amorphous Al-O phase surrounding (Co,Fe) grains provides a barrier for the diffusion of Co and Fe ions, thereby suppressing the crystal growth of Co-Fe alloy grains[15].

Figures 3(a) through (h) show TEM micrographs and selected area electron diffraction (SAD) patterns of as-deposited Co-Fe-Al-O thin films prepared at two different O_2 flow ratios of 6.63 % (Sample A) and 13.04 % (Sample B). The compositions of nano-grains of Sample A and B are those corresponding to $Co_{43}Fe_{40}Al_{15}O_2$ and $Co_{41}Fe_{38}Al_{13}O_8$ (in atomic %), respectively. It is seen from the planar TEM micrograph in Fig. 3(b) for Sample A that the microstructure is composed of large granules (dark dots) with a size of about 20 nm in an amorphous Al-O matrix (grey area). The cross-sectional TEM micrograph in Fig. 3(a) clearly shows a columnar growth of the granules. A clearer image of the (Co,Fe) grains can be seen from the planar high resolution TEM micrograph shown in Fig. 3(c). The value of ρ is rather low (57 μΩcm) for Sample A, indicating that (Co,Fe) grains are not completely isolated from the amorphous Al-O matrix. Rather, these grains are interconnected, although this is not clear from the TEM micrographs. The increase of the oxygen content causes a drastic change in the microstructure. The size of (Co,Fe) grains is much reduced, being 3~5 nm, and no columnar growth occurs. The value of ρ for Sample B is very high (374 μΩcm), indicating that each (Co,Fe) grain in this case is mostly isolated by the insulating Al-O amorphous phase. The HRTEM micrograph shown in

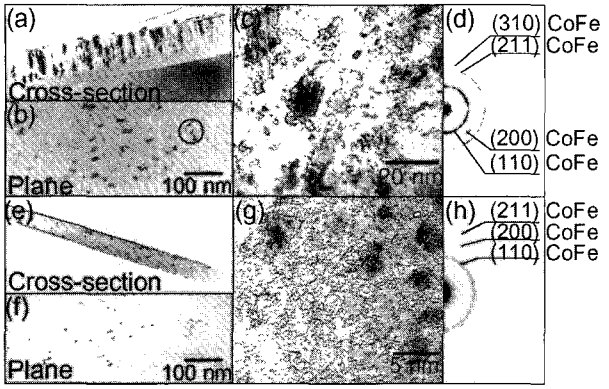

Fig. 3. TEM micrographs and SAD patterns are shown in (a) through (h). The results of as-deposited Co-Fe-Al-O films prepared at O_2 flow ratios of 6.63 % (Sample A) and 13.04 % (Sample B) are shown in (a) through (d), and (e) through (h), respectively.

Fig. 3(g) clearly shows this micro-structural feature. SAD patterns are shown in Figs. 3(d) and 3(h) for Sample A and B, respectively. The diffraction rings of the SAD patterns are consistent with those expected from the bcc (Co,Fe) phase. Note that the SAD patterns of Sample A with lower oxygen content (Fig. 3(d)) are sharper than those of Sample B (Fig. 3(h)). No SAD patterns related with oxide phases are observed, in agreement with the XRD results.

3.2 Electrical resitivity and magnetic properties

Figure 4(a) shows the results for ρ in as-deposited Co-Fe-Al-O granular films as a function of the O_2 flow ratio at various input powers of 100, 200 and 300 W, but at a fixed sputtering pressure of 5 mTorr. For a given O_2 flow ratio, ρ increases with decreasing input power, while, at a given input power, it increases with increasing O_2 flow ratio. This difference in ρ depending on the input power may be explained by the thermalization process. A sputtered light metal element, Al in this study, is considered to be highly thermalized in a high input power and is subjected to a high scattering, resulting in a low deposition rate[16]. As the input power increases, the amount of Al decreases, causing a low content of the Al-O phase. An abrupt increase in ρ occurs near an O_2 flow ratio of 20 % in the case of 200 W and 300 W. Possible reason for this is that the conductive path collapses near the O_2 flow ratio due to the percolation of the non-metallic, amorphous Al-O network[17].

The O_2 flow ratio dependence of $4\pi M_S$, H_K and coercivity (H_c) is shown in Fig. 4(b) for as-deposited Co-Fe-Al-O films fabricated at an input power of 200 W and a sputtering pressure of 5 mTorr. As the O_2 flow ratio

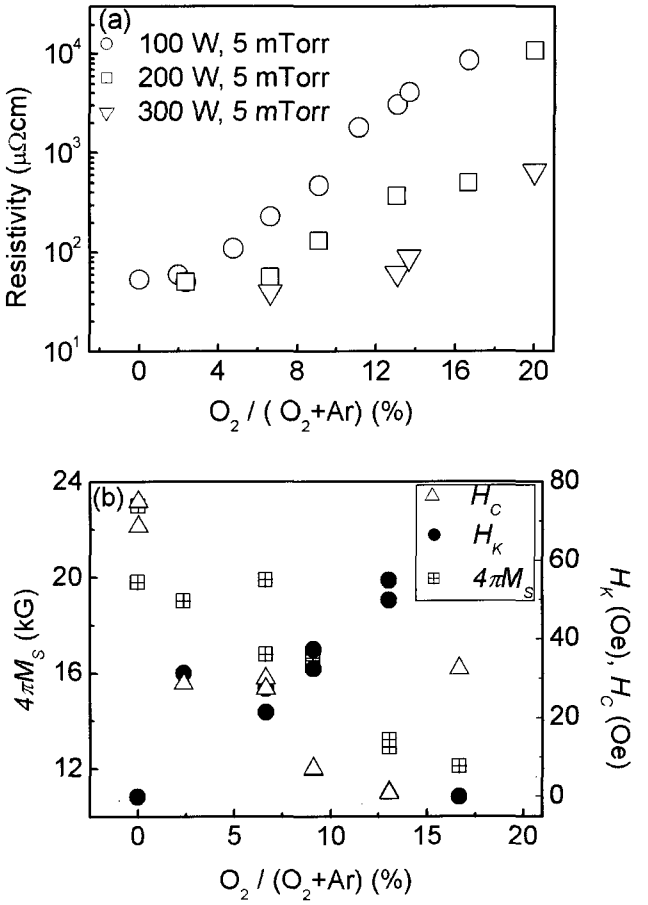

Fig. 4. (a) The magnitude of ρ of as-deposited Co-Fe-Al-O films as a function of the O_2 flow. (b) The values of $4\pi M_S$, H_K and H_c of as-deposited Co-Fe-Al-O films as a function of the O_2 flow ratio.

increases from 0 to 16.67 %, the value of 4 πM_s decreases monotonically from 23 to 11.9 kG, while the value of H_K increases from 0 to 55 Oe and then decreases again to 0 Oe at the highest O_2 flow ratio of 16.67 %. H_c tends to decrease with increasing O_2 flow ratio and shows a minimum at an O_2 flow ratio of 13.04 %. It is noted here that the values of 4 πM_s and ρ for Sample B are 12.9 kG and 374 μΩcm, respectively, a suitably high 4 πM_s being combined with a high ρ. The degradation of 4 πM_s with increasing the O_2 flow ratio is caused possibly by the formation of a non-magnetic phase at the outer region of the Co-Fe grains. This means that the oxidizing process takes place not only in the grain boundary but also in the grain itself. The decrease in H_C at the O_2 flow ratios of 13.04 % and below is due to the nano-crystallization of Co-Fe alloy grains. In the well-known random anisotropy model for nano-crystalline soft magnetic materials[18], H_C is proportional to the sixth power of the grain size. Note that H_C rapidly increases at O_2 flow

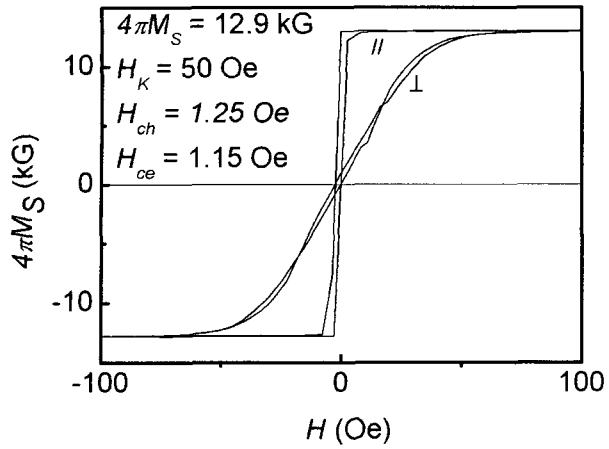

Fig. 5. Hysteresis loops of sample B, measured under in-plane fields applied in the directions parallel and perpendicular to the induced anisotropy.

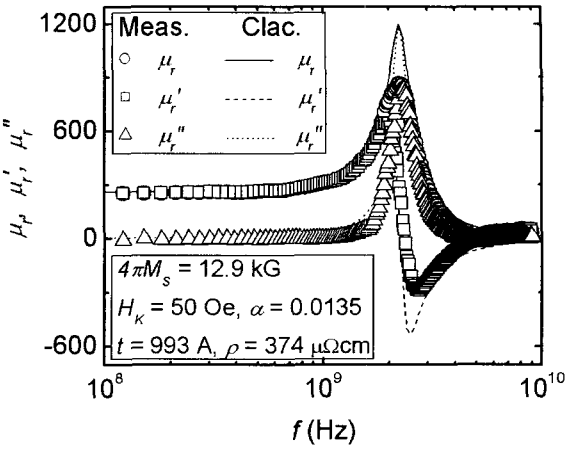

Fig. 6. Experimental (indicated by symbols) and theoretical (denoted by lines) spectra of the relative permeability for Sample B over a wide frequency range up to 9 GHz.

ratios above 13.04 %, possibly due to weak exchange coupling between ferromagnetic grains across a very thick non-magnetic Al-O amorphous phase. It is reminded that, in the random anisotropy model, exchange coupling among magnetic grains is essential to the reduction of the effective magneto-crystalline anisotropy[18].

As was mentioned previously, the following relation exists among f_R, 4 πM_S, and H_K; $f_R = (\gamma/2\ \pi)(4\ \pi M_S\ H_K)^{1/2}$. 4 πM_s and H_K are two important factors for f_R. In this study, the films were deposited in a static field as high as 1 kOe to induce a large uniaxial anisotropy. A static field of 1 kOe during sputtering, which was made possible with a specially designed sample holder, is considered to be high enough to completely saturate the sample, because this magnitude of applied field is much larger than the coercivity of the samples. However, induced anisotropy is not always formed; for example, at a fixed sputtering pressure of 5 mTorr, the induced anisotropy is not formed at input powers of 100 and 300 W, but it is formed at an intermediate input power of 200 W. Although the precise reason for this is not clearly known at this moment, it seems somewhat related with the microstructure. Detailed micro-structural investigation shows that nano-crystalline grains with a grain size smaller than approximately 5 nm are only observed at an input power of 200 W (and also at a suitable oxygen flow ratio). Pair ordering is known to be the reason for the induced anisotropy. This means that atomic diffusion should occur during deposition in order for the induced anisotropy to be formed. In general, atomic diffusion in bulk crystals is (much) lower than that in amorphous phase or grain boundary. This mainly explains the well-known fact that the induced anisotropy is more easily formed and also its magnitude is generally larger in amorphous materials. The large induced anisotropy observed in this study for thin films with ultra-small grains can similarly be explained. With nano-crystalline grains whose grain size is in the range of 5 nm, there is a significant portion of grain boundary, resulting in enhanced atomic diffusion. In Fig. 4(b), considering the relationship between H_K and the O_2 flow ratio, the induced anisotropy reaches a maximum value at 13.03 % and then suddenly decreases above 13.03 %.

Hysteresis loops of Sample B, measured under in-plane fields in the directions parallel and perpendicular to the induced anisotropy, are shown in Fig. 5. Important magnetic properties are; 4 πM_S = 12.9 kG, H_K = 50 Oe, H_{ch} (in the perpendicular, hard direction) = 1.25 Oe, and H_{ce} (in the parallel, easy direction) = 1.15 Oe. The thin film indeed exhibits a very good magnetic softness, combined with high values of 4 πM_S and H_K, which are important parameters for f_R.

Figure 6 shows the results for experimental (indicated by symbols) and theoretical (denoted by lines) spectra of the relative permeability for Sample B. The scanned frequency range is very high, being up to 9 GHz. The effective permeability and both the real and imaginary parts of the permeability are shown in the figure. The theoretical permeability spectra are computed by using the Landau-Lifshitz-Gilbert equation. There are 5 input parameters in the equation: 4 πM_S, H_K, ρ, the film thickness (t) and damping constant (α). Among these, α is only the fitting parameter, the rest being taken from the present experimental results. The agreement between the experimental and theoretical results is reasonable in most cases. The damping constant extracted from the fit is 0.0135 and this magnitude of damping is considered to be reasonable in this kind of materials. During the

permeability measurements, the exciting field was applied in the direction perpendicular to the easy axis. The real part of the permeability (μ') is nearly flat up to 1 GHz and, in this frequency range, the imaginary part of the permeability is very low. The imaginary part (μ'') shows a peak at f_R (=2.24 GHz). The measured value of the (pseudo) dc permeability is 260, and this value is in excellent agreement with the calculated value of 258 based on the rotation magnetization mechanism. This agreement indicates that the magnetization mainly occurs by spin rotation.

3.3 RF electromagnetic-noise filter applications

Sample B was chosen and tested as an RF noise filter. Important properties of Sample B are as follows; ρ = 374 μΩcm, H_K = 50 Oe, H_{ch} = 1.25 Oe, $4\pi M_S$ = 12.9 kG and f_R = 2.24 GHz. The real part of the measured relative permeability is 260 at low frequencies and this value is maintained up to 1 GHz.

The present CPW transmission line device (see Fig. 1) consists of 3 parallel Cu lines and the line at the center is the signal line and the rest are the ground lines. A magnetic film is mounted on top of the CPW line to absorb unwanted noise. Figure 7(a) shows the frequency dependence of the transmitted (S_{21}) and reflected (S_{11}) scattering parameters for a non-integrated CPW transmission line incorporated with the present Co-Fe-Al-O thin film. The noise attenuation caused by a dielectric loss is smaller than that by FMR and eddy current losses[1,2]. The FMR and eddy current losses are therefore considered as the main sources of noise attenuation. In order to use the FMR loss as the noise attenuation, the easy axis of the magnetic film should be parallel to the direction of the wave propagation ($\boldsymbol{h}_{rf}$) in the CPW transmission line (see Fig. 1(b)). The insertion loss of the present Co-Fe-Al-O incorporated CPW transmission line, which can be obtained from the frequency dependence of S_{21}, is very low (less than 0.3 dB) and this value is maintained up to 2 GHz. The degree of noise suppression (intensity of S_{21} parameter) is about 3 dB up to 20 GHz. A minimum in the frequency dependence of S_{21} is observed at 3.3 GHz. At the same frequency, a maximum in S_{11} occurs. The value of S_{11} is maintained very low being lower than -30 dB up to 2 GHz, above which it rapidly increases reaching a maximum at 3.3 GHz. These maximum and minimum peaks in the frequency dependence of S_{11} and S_{21} are probably due to the FMR loss of the Co-Fe-Al-O film placed on top of the CPW line. This value of f_R is substantially higher than that of 2.24 GHz obtained with a pick-up coil type permeameter (see Fig. 6). Considering the exactly same sample (including the dimensions) in both cases, this disagreement appears somewhat strange. With the lateral dimensions of 4 mm × 4 mm, there should not be any substantial shape

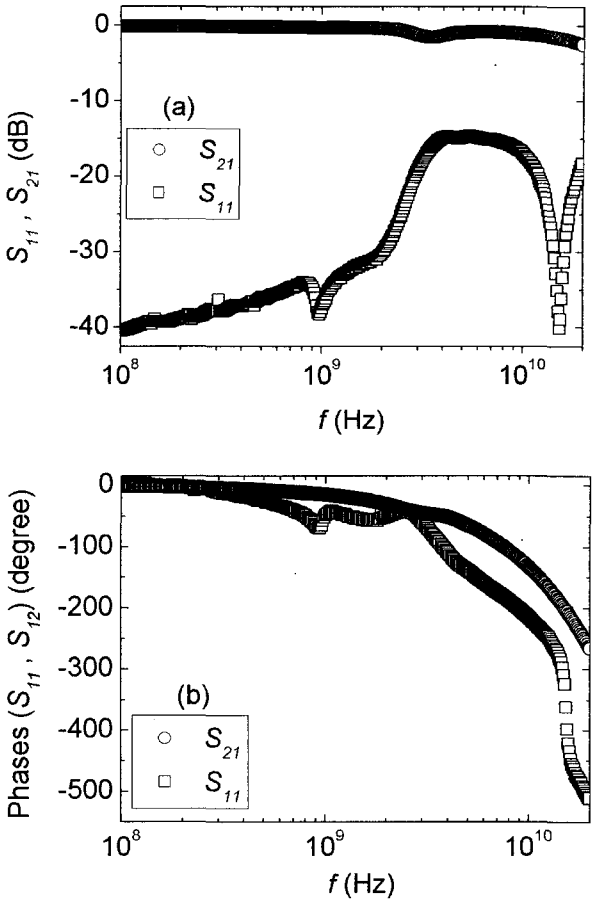

Fig. 7. The frequency dependence of (a) the transmitted (S_{21}) and reflected (S_{11}) scattering parameters and (b) the phase shifts of S_{21} and S_{11} for a non-integrated CPW transmission line incorporated with a Co-Fe-Al-O thin film.

anisotropy in the present sample. However, it is found that there exists an effective shape anisotropy due to the geometry of the CPW transmission line. Although essentially no shape anisotropy is expected from the present sample dimensions, the field generated from the CPW signal line is very much localized, resulting in localized magnetization and hence shape anisotropy. This is clearly supported from a finite element method (FEM) computer simulation with a commercial simulation package (HFSS Version 8.5). Some of the results are shown in Fig. 8, where the magnetic field direction of the Co-Fe-Al-O incorporated CPW transmission line is displayed at an FMR frequency of 3.3 GHz. A practically useful magnetic field to magnetize the incorporated film is distributed along the center transmission line (the signal line). The area of localized magnetization is very small and also it has a very high aspect ratio (50~65 μm in width × 2 mm in length), resulting in a high effective shape anisotropy.

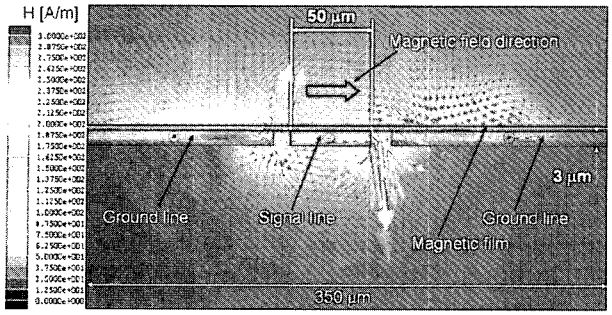

Fig. 8. The direction of magnetic field generated from the CPW transmission line incorporated with a 0.1 μm thick Co-Fe-Al-O film with a resonance frequency of 3.3 GHz.

In addition to the maximum peak in the frequency dependence of S_{11}, there are two minimum peaks observed at about 1 and 15 GHz. The peak at 15 GHz is considered to be due to a dimensional loss, often observed previously[19-22], but the origin for the peak at 1 GHz is not clear yet. According to the electrical length principle (or so-called the quarter wave length rule)[19-22], the dimensional loss is closely related to the length of a magnetic film mounted onto a transmission line. In order to avoid dimensional losses, the length of a magnetic film should be less than the quarter wavelength of the highest operating frequency. The length of the Co-Fe-Al-O magnetic film used in this study is 4 mm which is greater than the quarter wavelength (3.75 mm) at 20 GHz.

In Fig. 7(b), the frequency dependence of the phase-shift is shown for S_{11} and S_{21}. A minimum peak in the frequency dependence of the phase-shift in S_{21} is observed at 3.3 GHz, the same frequency for the FMR peak observed in the frequency dependence of S_{21} (Fig. 7(a)). Although the peak intensity is not as significant as that observed in the frequency dependence of S_{21}, this peak is due to the FMR loss. One maximum and two minimum peaks are observed in the frequency dependence of the phase-shift in S_{11}, similarly to the frequency dependence of S_{11}.

Two points can be noted from the results shown in Figs. 7(a) and (b). One is that the intensity of the reflected signal rapidly increases and its phase-shift decreases as the FMR occurs. The behavior of the transmitted signal is just opposite; namely, the intensity of the transmitted signal decreases and its phase-shift increases. The other point is that the present Co-Fe-Al-O film is potentially very suitable for a low-frequency pass-band filter with a pass-band up to 2 GHz.

Figure 9(a) again shows the frequency dependence of S_{21} for the present non-integrated CPW transmission line incorporated with the Co-Fe-Al-O thin film, mainly to

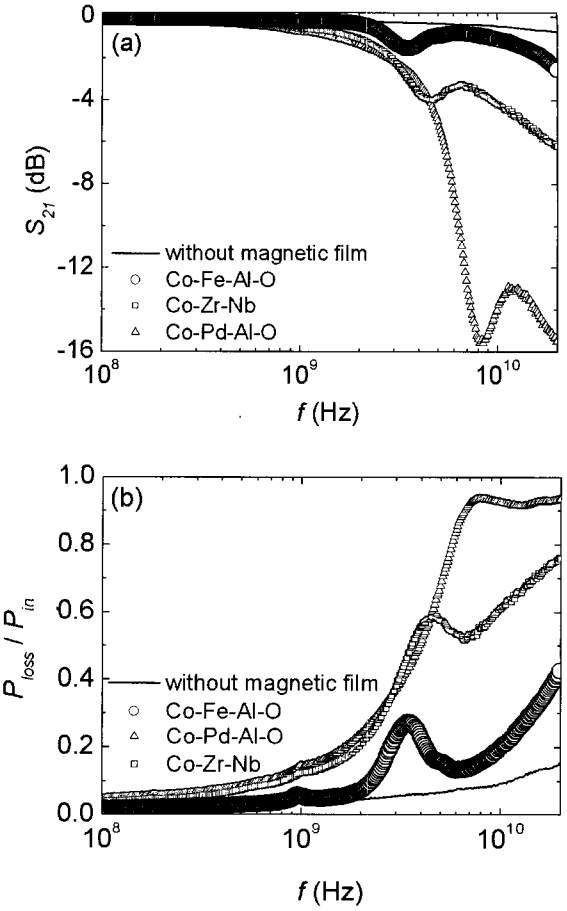

Fig. 9. The frequency dependence of (a) the transmitted scattering parameter (S_{21}) and (b) the power loss for a non-integrated CPW transmission line incorporated with a Co-Fe-Al-O thin film.

compare the present results with those for the bare CPW transmission line (no magnetic thin film incorporated) and other non-integrated noise suppressors using Co-Zr-Nb and Co-Pd-Al-O magnetic films[1]. The noise attenuation of 3 dB up to 20 GHz for the Co-Fe-Al-O film incorporated CPW line is small compared with the attenuation observed in the Co-Zr-Nb and Co-Pd-Al-O incorporated suppressors[1,2]. However, considering that the volume of the Co-Fe-Al-O film on the CPW transmission line is about 38 times smaller than that of Co-Zr-Nb and Co-Pd-Al-O films, the S_{21} value of 3 dB achieved in this work is considered to be not small.

The degree of noise suppression is reported to be proportional to the volume of a magnetic film mounted on a CPW transmission line[1,2]. Note that the dimensions of Co-Zr-Nb and Co-Pd-Al-O magnetic films on CPW transmission lines are 15 mm × 2 mm × 2 μm and those of the signal line are 15.2 mm × 50 μm × 3 μm. Note also that, in both cases, a polyimide-insulation

layer with thickness of 7.5 μm was disposed between the magnetic film and the CPW transmission line and, for enhanced proximity, a mechanical pressure was applied on the incorporated magnetic films during the measurement. On the other hand, no pressure was intentionally applied for the Co-Fe-Al-O incorporated CPW transmission line. The attenuation characteristics are expected to improve with an applied pressure. The results shown in Fig. 9(a) were obtained for non-integrated devices. The most common and efficient way of enhancing the proximity is to integrate the Co-Fe-Al-O film on the CPW line.

Figure 9(b) shows the frequency profile of the power loss of the Co-Fe-Al-O incorporated CPW transmission line. Similar results for Co-Zr-Nb and Co-Pd-Al-O incorporated structures and the bare transmission line are also shown for comparison. A large loss peak appears at 3.3 GHz, which is identical to the minimum of the attenuation (Fig. 7(a)). This loss peak is therefore due to the FMR loss generation. The other noise filters with larger magnetic volume show a high degree of loss generation. A large loss generation is expected when the volume of the present nano-granular Co-Fe-Al-O magnetic film is large. It is particularly noted that, below 2 GHz (a possible pass-band), the insertion loss of the present device is as small as the bare transmission line. It implies that the Co-Fe-Al-O film with a high ρ is a good candidate for an RF noise filter even without an insulator layer between the magnetic thin film and the CPW transmission line. Work is currently under way to improve the noise suppression characteristics. Some parameters under consideration are the sample dimensions and the width of the signal line (which may affect the magnitude and frequency range of power loss generation).

4. CONCLUSION

Co-Fe-Al-O nano-granular films with excellent soft magnetic properties at high-frequencies were fabricated by RF magnetron reactive sputtering. A systematic investigation on the microstructure, electrical, and magnetic properties indicates a large role of the oxygen content in the thin films. Important electrical and magnetic properties of a typical thin film with the composition (in atomic %) $Co_{41}Fe_{38}Al_{13}O_8$ are; 374 μΩcm (ρ), 12.9 kG ($4\pi M_S$), 50 Oe (H_K), 1.25 Oe (H_{ce}), and 1.15 Oe (H_{ch}), 260 (μ') and 2.24 GHz (f_R). A non-integrated type CPW transmission line incorporated with the Co-Fe-Al-O thin film with the dimensions of 4 mm × 4 mm × 0.1 μm exhibits good noise suppression properties; the insertion loss is very low being less than 0.3 dB and this value is maintained over 2 GHz, a possible pass-band, and the degree of noise suppression is 3 dB up to 20 GHz. The absolute magnitude of the attenuation is considered to be not high enough for real applications, but this can be increased by increasing the magnetic volume and integrating the magnetic thin film into the CPW transmission line. Work is in progress toward this direction.

REFERENCES

[1] K. H. Kim, M. Yamaguchi, K. I. Arai, H. Nagura, and S. Ohnuma, "Effect of radio-frequency noise suppression on the coplanar transmission line using soft magnetic thin films", J. Appl. Phys., Vol. 93, No. 10, p. 8002, 2003.

[2] K. H. Kim, M. Yamaguchi, S. Ikeda, and K. I. Arai, "Modeling for RF noise suppressor using a magnetic film on coplanar transmission line", IEEE Trans. Magn., Vol. 39, No. 5, p. 3031, 2003.

[3] M. Fujimoto, "Inner stress induced by Cu metal precipitation at grain boundaries in low-temperature-fired Ni-Zn-Cu ferrite", J. Am. Ceram. Soc., Vol. 77, No. 11, p. 2873, 1994.

[4] M. Fujimoto, K. I. Hoshi, M. Nakazawa, and S. Sekiguchi, "Cu multiply twinned particle precipitationin low-temperature fired Ni-Zn-Cu ferrite", Jpn. J. Appl. Phys., Vol. 32, p. 5532, 1993.

[5] M. Fujimoto, T. Suzuki, Y. Nishi, K. Arai, and S. Sekiguchi, "Coherent precipitation of copper metal in low-temperature-fired Ni-Zn-Cu ferrite", J. Am. Ceram. Soc., Vol. 81, p. 2477, 1998.

[6] M. Yamaguchi, K. Suezawa, K. I. Arai, Y. Takahashi, S. Kikuchi, Y. Shimada, S. Tananbe, and K. Ito, "Magnetic thin-film inductors for RF-integrated circuits", J. Magn. Magn. Mater., Vol. 215-216, p. 807, 2000.

[7] M. Yamaguchi, K. Suezawa, K. I. Arai, Y. Takahasi S. Kikuchi, Y. Shimada, W. D. Li, S. Tanabe, and K Ito, "Microfabrication and characteristics of magnetic thin-film inductors in the ultrahigh frequency region", J. Appl. Phys., Vol. 85, p. 7919, 1999.

[8] W. D. Li, K. Kato, O. Kitakami, and Y. Shimada, "Anisotropy of highly resistive soft magnetic Fe-Al-O granular films", J. Magn. Soc. Jpn., Vol. 22, No. 4-2, p. 442, 1998.

[9] H. J. Lee, S. Mitani, T. Shima, S. Nagata, and H. Fujimori, "Permeability properties of highly resistive Fe-Al-O films", J. Magn. Soc. Jpn., Vol. 23, No. 1-2, p. 246, 1998.

[10] Y. Yosizawa, S. Oguma, and K. Yamaguchi, "New Fe-based soft magnetic alloys composed of ultrafine grain structure", J. Appl. Phys., Vol. 64, No. 10, p. 6044, 1988.

[11] S. Ohnuma, H. Fujimori, S. Mitani, and T. Masumoto, "High-frequency magnetic properties in metal-nonmetal granular films", J. Appl. Phys., Vol. 79, No. 8, p. 5130, 1996.

[12] S. Ohnuma, N. Kobayashi, T. Masumoto, S. Mitani, and H. Fujimori, "Soft magnetic properties of Co-Fe-Al-O thin films with high B_S", J. Magn. Soc. Jpn., Vol. 23, No. 1-2, p. 240, 1999.

[13] S. Ohnuma, N. Kobayashi, T. Masumoto, S. Mitani, and H. Fujimori, "Magnetostriction and soft magnetic properties of $(Co_{1-x}Fe_x)$-Al-O granular films with high electrical resistivity", J. Appl. Phys., Vol. 85, No. 8, p. 4574, 1999.

[14] B. C. Wadell, "Transmission line design handbook", Norwood, MA: Artech House, 1991.

[15] J. C. Sohn, D. J. Byun, and S. H. Lim, "Nano-granular Co-Fe-Al-O sputtered thin films for magnetoelastic device applications in the GHz frequency range", J. Magn. Magn. Mater., Vol. 272-276, p. 1500, 2004.

[16] K. Ikeda, K. Kobayashi, and M. Fujimoto, "Microstructure and magnetic properties of (Co-Fe)-Al-O thin films", J. Am. Ceram. Soc., Vol. 85, No. 1, p. 163, 2002.

[17] M. Ohnuma, K. Hono, H. Onodera, S. Ohnuma, H. Fujimori, and J. S. Pedersen, "Microstructure and magnetic properties of Co-Al-O granular thin films", J. App. Phys., Vol. 87, No. 2, p. 817, 2000.

[18] H. Fujimori, S. Mitani, T. Ikeda, and S. Ohnuma, "High electrical resistivity and permeability of soft magnetic granular alloys", IEEE Trans. Magn., Vol. 30, p. 4779, 1994.

[19] G. Herzer, "Grain size dependence of coercivity and permeability in nano-crystalline ferromagnets", IEEE Trans. Magn., Vol. 26, No. 5, p. 1397, 1990.

[20] W. Barry, "A broad-band, automated, stripline technique for the simultaneous measurement of complex permittivity and permeability", IEEE Trans. Microwave Theory Tech., Vol. MTT-34, No. 1, p. 80, 1986.

[21] W. B. Weir, "Automatic measurement of complex dielectric constant and permeability at microwave frequencies", Proc. IEEE, Vol. 62, p. 33, 1974.

[22] A. M. Nicolson and G. F. Ross, "Measurement of the intrinsic properties of materials by time-domain techniques", IEEE Trans. Instrum. Meas., Vol. IM-19, No. 4, p. 377, 1970.

[23] R. W. Ziolkowski, "Design, fabrication, and testing of double negative metamaterials", IEEE Trans Antennas Propagat., Vol. 51, No. 7, p. 1516, 2003.